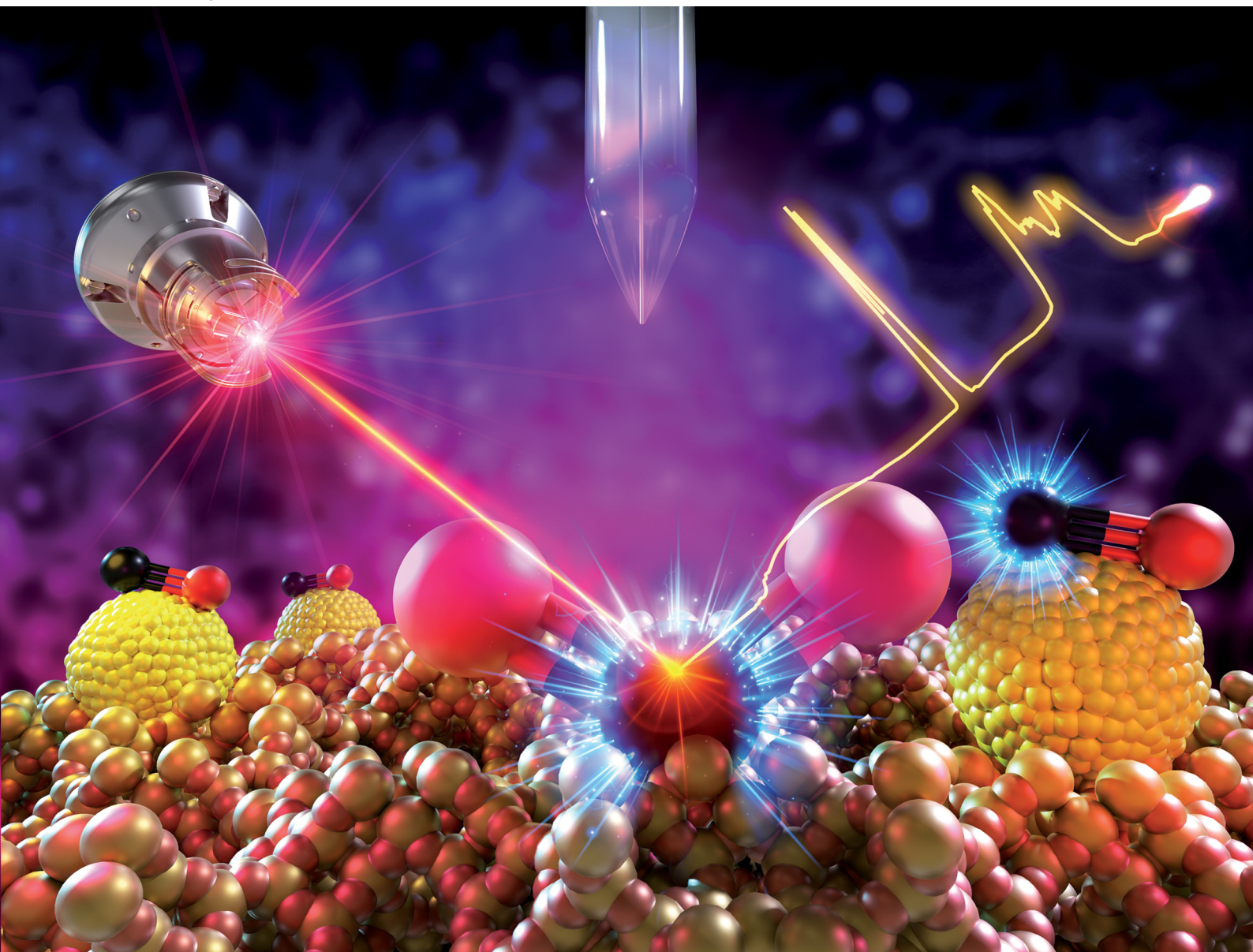


EES Catalysis

rsc.li/EESCatalysis



ISSN 2753-801X

PERSPECTIVE

Calvin Mukarakate *et al.*
Exploring opportunities in *operando* DRIFTS and
complementary techniques for advancing plasma catalysis



Cite this: *EES Catal.*, 2024,
2, 1059

Exploring opportunities in *operando* DRIFTS and complementary techniques for advancing plasma catalysis†

Stefano Dell'Orco,^a Noemi Leick,^b Jeffrey L. Alleman,^b Susan E. Habas^a and Calvin Mukarakate^{*,a}

Exploring the dynamic interaction of non-thermal plasma (NTP) with catalytic processes is critical to unravelling elusive catalyst structure–function relationships under NTP conditions, specifically dielectric barrier discharges (DBD). This study investigates the efficacy of *operando* diffuse reflectance infrared Fourier transform spectroscopy (DRIFTS) as a tool for characterizing intermediates created by NTP on catalyst surfaces. Leveraging insights from traditional DRIFTS in thermochemical catalysis, we explore the complexities of plasma-induced catalytic reactions, discussing both opportunities and limitations of DRIFTS to study these reaction mechanisms. By summarizing findings from literature and addressing existing knowledge gaps, this perspective highlights how different DRIFTS configurations can affect results, stressing the importance of establishing best practices for studying DBD-driven reactions with DRIFTS. The intended outcomes of this work are to provide guidance on how to effectively use DRIFTS, share fundamental insights into DBD-assisted catalysis, and emphasize the need for complementary techniques to develop catalysts suited for NTP environments.

Received 24th April 2024,
Accepted 8th July 2024

DOI: 10.1039/d4ey00088a

rsc.li/eescatalysis

Broader context

In the quest for sustainable energy and chemicals, the conversion of low-energy molecules such as water, carbon dioxide, and methane into valuable chemicals and fuels represents a significant challenge. The anticipated increase in renewable electricity availability further emphasizes the importance of electrifying chemical and fuel synthesis processes to significantly reduce greenhouse gas emissions. Non-thermal plasma (NTP) coupled with heterogeneous catalysis holds promise in enabling otherwise thermodynamically unfavorable reactions by energizing electrons. However, understanding the intricate interaction between plasma and catalysts still represents a challenge for developing novel catalyst formulations that enhance product selectivity and efficiency. In this context, *operando* diffuse reflectance infrared Fourier transform spectroscopy (DRIFTS) serves as a crucial analytical tool in unraveling the complexities of plasma-induced catalytic reactions, providing insights into the intermediates created by NTP on catalyst surfaces and elucidating reaction mechanisms under NTP conditions. Addressing the knowledge gap between plasma physics and catalyst development is crucial for advancing NTP-driven pathways in sustainable energy and chemicals. Thus, we present recent significant efforts on NTP-modified DRIFTS cells, providing guidance on best practices for DRIFTS usage and advocating for the use of complementary techniques to deepen the understanding of reaction mechanisms for catalysis development.

1. Introduction

Recently, non-thermal plasma (NTP) has gained widespread attention for its unique characteristics and versatile applications across various scientific disciplines.¹ NTP, characterized by high electron temperatures compared to gas temperatures,

holds promise for synthesizing fuels and chemicals from renewable and waste carbon sources.² One common form of NTP is the dielectric barrier discharge (DBD), generated by applying a potential difference across two electrodes separated by a dielectric material. This system induces an electric field that partially ionizes the gas, producing positive ions and electrons while leaving many molecules neutral. Electron-impact collisions with gas molecules result in ionization, vibrational and electronic excitation, and dissociation processes. These collisions can produce new electrons, sustaining the plasma, and result in light emission when excited molecules return to a lower energy level. There are two possible types of DBD systems: alternating current (AC) and radio frequency

^a Catalytic Carbon Transformation & Scale-up Center, National Renewable Energy Laboratory, 15013 Denver West Parkway, Golden, CO 80401, USA.

E-mail: Calvin.Mukarakate@nrel.gov

^b Materials, Chemical, and Computational Science Directorate, National Renewable Energy Laboratory, 15013 Denver West Parkway, Golden, CO 80401, USA

† Electronic supplementary information (ESI) available. See DOI: <https://doi.org/10.1039/d4ey00088a>



(RF) plasmas, differing in the frequency of the applied electric field. AC plasma operates at frequencies below 100 kHz, while RF plasma operates at frequencies between 100 kHz and several MHz, offering higher power densities and more efficient plasma generation.³ The plasma discharges can either be filamentary or continuous (glow discharge) depending on the gas composition, pressure, and applied voltage. The presence of reactive species is what makes DBD plasmas an interesting approach to activate gas molecules, especially through dissociation.⁴

Many applications of NTP, including DBD plasmas, require catalysts to tailor selectivity toward specific target products, leading to a growing interest in plasma catalysis that leverages NTP-relevant catalyst features to enhance catalytic reactions.^{1,5} Therefore, plasma catalysis, which integrates NTP with catalytic processes, has emerged as a promising field, offering both opportunities and challenges that necessitate further investigation to refine tailored catalyst materials for optimal performance in NTP-driven reactions.^{6,7} Typically, plasma catalysis, as for thermo-catalysis, involves a heterogeneous catalytic process where a solid catalyst, such as a transition metal on a support (*e.g.*, metal oxide), is used to facilitate the transformation of reactive gases on the catalyst surfaces. Adsorbed species may undergo surface reactions *via* Langmuir–Hinshelwood or Eley–Rideal mechanisms.⁸ One benefit of plasma catalysis is the ability for ionized, excited species (*i.e.* vibrationally and electronically excited species), radicals and dissociated species to interact with a catalyst at near-ambient temperatures, a condition where traditional thermal catalysis would typically not be effective.⁹

In situ and *operando* infrared (IR) spectroscopy is a very useful technique to study surface species to inform reaction mechanisms. Transmission IR is particularly useful because it not only enables identification of surface species relevant to reaction mechanisms but also allows quantification of such species. However, it can be challenging to utilize this technique for absorbing and/or scattering catalysts. While transmission IR is commonly used for a broad range of research,^{10–12} Diffuse reflectance infrared Fourier transform spectroscopy (DRIFTS) has become one of the most widely adopted techniques in catalysis research based on the ease of use, simple sample preparation, and commercial availability of *in situ* reactors that enable heating and gas flow through a catalyst bed. The extensive use of thermal DRIFTS for the characterization of surface species to inform reaction mechanisms and catalyst development provides valuable insights into the utility of the technique for plasma catalysis.^{13–17} DRIFTS can play a pivotal role in elucidating existing knowledge gaps in plasma catalysis by: (a) identification and quantification of species on catalyst surfaces, (b) evaluation of the effect of gas-phase plasma species on the chemistry at the catalyst surface, (c) determination of NTP-induced reaction mechanisms at the catalyst surface, and (d) differentiation of thermal and plasma-driven catalysis.

This perspective explores the opportunities and limitations of DRIFTS in advancing plasma catalysis, focusing on its role in

tracking surface chemistry during NTP-catalyzed reactions. Specifically, we focus on DBD configurations to generate NTP as these are the most highly studied systems. Given the diverse nature of modified DBD DRIFTS cells, we use the denomination *operando* to highlight that the reaction mechanisms were investigated under operating conditions. When it is unknown or unclear, the more general term *in situ* is used.¹⁸ We review results and observations reported by researchers using DRIFTS in the presence of NTP, highlighting its use to propose reaction mechanisms during plasma catalysis. Custom designed DRIFTS cells incorporating DBD can be classified into two main categories: those that embed the power electrode in the catalyst bed or those that orient the power electrode over the catalyst bed. In both cases, *in situ* configurations are possible since the IR signal is not intercepted or disturbed by the plasma itself, assuming the electrode does not obstruct the IR beam. Additionally, NTP does not have IR components in the range of interest of adsorbate species that would dominate the IR spectrum. These different configurations will be discussed in detail, emphasizing the impact of the electrode location relative to the catalyst. The utility of DRIFTS to address existing knowledge gaps in plasma catalysis, such as coupling solid catalysts with NTP, is discussed as is the need for complimentary techniques to obtain a comprehensive understanding of reaction mechanisms. The goal of this work is to explore comprehensively DRIFTS in the context of plasma catalysis, elucidating both advantages and limitations. This study aims to advance fundamental knowledge and facilitate practical implementation of plasma catalysis for diverse applications, providing valuable guidance for future research.

2. Results and discussion

2.1 Catalyst development informed by DRIFTS in thermochemistry

In situ DRIFTS is very effective in helping to elucidate reaction mechanisms for thermochemical catalytic reactions, since it is able to measure the vibrational fingerprint of surface adsorbates.^{19,20} The technique is particularly beneficial when these adsorbates are bound to materials that strongly absorb IR radiation with complex surfaces or coatings, as well as powders with high surface areas that scatter incoming radiation. Additionally, the ease of sample preparation and the *in situ* capabilities of most commercially available cells allows investigation of relevant pressure and temperature conditions. However, DRIFT spectra are very sensitive to experimental conditions and therefore face difficulties in achieving quantitative information. In DRIFT spectroscopy, incident IR beams can be reflected at particle surfaces at the top layer of the catalyst bed, leading to specular reflection. Diffuse reflection originates from IR radiation being reflected by multiple particles in the bed, as depicted in Fig. 1. The reflected signal contains information about the catalyst itself (*i.e.*, the particles) and the surface adsorbates which are of prime interest in DRIFTS measurements. When diffuse reflection is



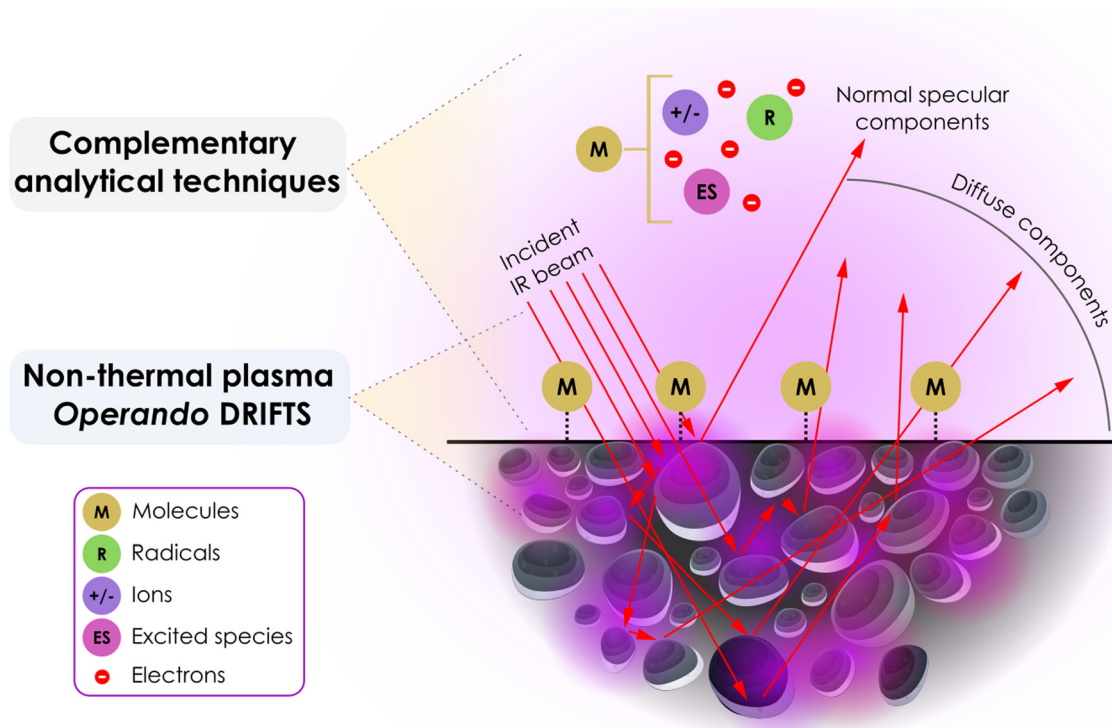


Fig. 1 Processes responsible for producing the diffuse reflected infrared spectrum of adsorbates on a powder catalyst. Purple regions represent schematically the presence of local plasma discharge zones, while red arrows represent infrared beam lines. Modified from Armaroli *et al.*¹⁹

predominant over specular reflection, DRIFTS yields spectra akin to transmission spectra, yet with much weaker intensity. The contribution of specular reflection remains a primary cause of DRIFT spectra distortion. Material properties such as refractive index, particle dimensions, packing density, homogeneity, and absorption coefficients influence the quality of the DRIFT spectra. Ideally, the particle size should be $< 10 \mu\text{m}$, and if the sample is highly absorbent, dilution in a nonabsorbent matrix, such as KCl or KBr, can promote deeper light penetration and increase the diffuse reflection contribution of the signal.

Due to the complexity of the DRIFT signal, the Lambert-Beer law applied in transmission mode is not directly applicable. For highly absorbing samples, the Kubelka-Munk (K-M) equation provides an alternative way to obtain a spectrum similar to a transmission spectrum, and in the case of weakly absorbing samples, the DRIFT spectrum is best represented as absorbance ($\log(1/R)$) where R denotes the sample reflectance. Additionally, the same catalyst sample and conditions may not yield the same DRIFT spectra as reproducibility challenges arise due to variations in diffusion coefficients between preparations. Spectra normalization to iso-intensity of a characteristic structure band of a bonded species helps mitigate this issue. This normalization process effectively ensures that any observed differences in spectra are more likely to be attributed to variations in surface species or functional groups rather than experimental variability.¹⁹

To inform the catalytic mechanism, surface analysis through DRIFTS alone may be insufficient, necessitating the examination of gases leaving the DRIFTS cell using downstream gas analysis through IR spectroscopy, gas chromatography (GC), or mass spectrometry (MS). Combining DRIFTS with complementary techniques (as later discussed in Section 2.3) can provide additional benefits in deepening the understanding of the reaction mechanism in terms of surface distribution of intermediates as well as near surface radicals and activation energies. Therefore, surface analysis through DRIFTS only can be a major drawback for understanding plasma catalysis. As illustrated in Fig. 2, in certain configurations, the plasma zone may not coincide with the surface probed by the IR radiation. Depending on the configuration, and the distance of the plasma zone from the catalyst surface and bulk, the plasma-catalyst interactions will differ as will the species observed by each characterization technique. Recently, plasma-assisted catalytic CO_2 hydrogenation has gained significant interest and thanks to the large IR cross-sections of adsorbed CO_2 and CO , and their sensitivity to co-adsorbates and local environmental factors, DRIFTS has demonstrated utility in helping to understand reaction mechanisms and informing catalyst design.²¹⁻²⁶ Therefore, we will discuss the benefits and limitations of DRIFTS for plasma catalysis using CO_2 hydrogenation as a probe reaction along with CH_4 oxidation, dry reforming of methane, and selective catalytic reduction of hydrocarbons.



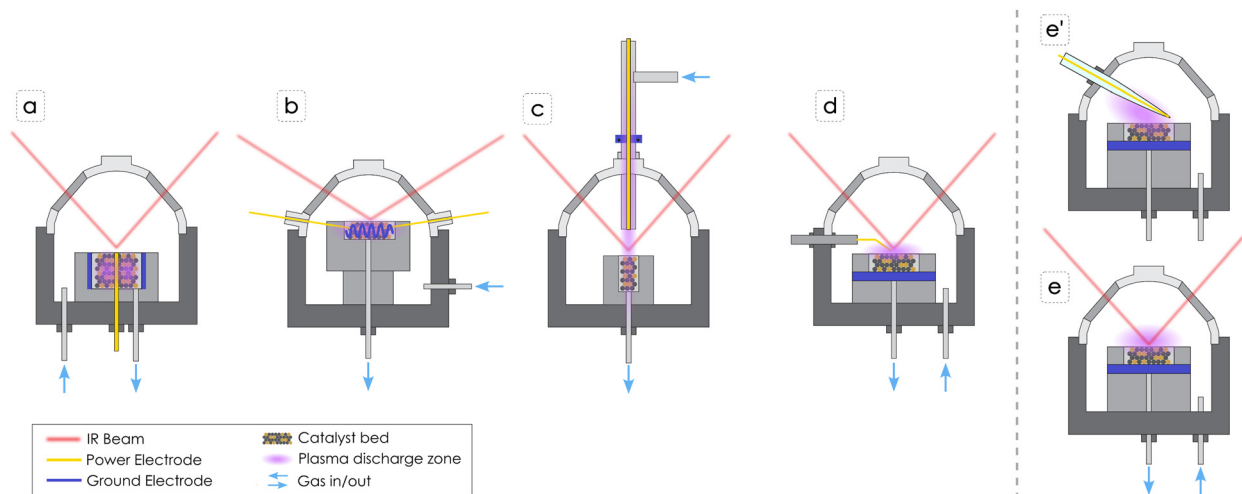


Fig. 2 Schematic of *operando* DRIFTS configurations developed by research groups for investigating plasma catalysis under reaction conditions. (a) DBD embedded within the catalyst bed, (b) helical surface DBD, (c) DBD above the catalyst bed, (d) point-source DBD, (e) and (e') point-source DBD with two different views (this study). The dielectric is: (a) the quartz capillary covering the power electrode, (b) a coating on the power electrode, (c) the quartz tube containing the plasma discharge zone, (d) the sample holder depicted in light grey, (e) and (e') the quartz tube covering the power electrode tip.

2.2 Plasma-catalyst interactions in DBD-driven chemistry

Unlike thermal catalysis, NTP generates reactive species in the gas phase through electron-impact events, creating ionized species, excited species, and radicals that can interact with catalyst surfaces, enabling new reaction pathways or chemistries that would otherwise be thermodynamically unfavorable. Generally, the lifetime of activated gas-phase species is short, ranging from a few nanoseconds for electronically excited species to microseconds and seconds for radicals. Besides enabling chemistry, energized species from the plasma zone can impact the catalyst surface leading to etching through physical sputtering and causing changes in the catalyst structure, or they can cause chemical reactions such as dissociation or desorption of surface species. Every plasma reactor, including DBD DRIFTS systems, has its own electric circuit with a defined impedance and a specific power supply, therefore the applied voltage and frequency can be different. Most of the studies included here utilize AC plasma generators, except one that generates plasma through an RF. The applied voltage and frequency, and plasma generator impacts the actual power transferred to the gases, as does the choice of gas composition. The breakthrough voltage refers to the minimum voltage required to initiate plasma discharge in a gas, and it can vary depending on the experimental system, the gas composition, pressure, and electrode configuration. Therefore, some gases, such as argon (Ar), are easier to ionize into plasma compared to CO₂, due to a lower ionization energy. As a result, some researchers used a dilution gas, such as Ar, to ignite and stabilize the plasma. The applied voltage differs from the injected voltage into the plasma discharge (and therefore the power differs) due to losses in voltage transmission and coupling into the gas phase. Consequently, it is important to properly measure and report plasma generation details.

DRIFTS cells specifically tailored for *in situ* plasma catalysis studies can play a pivotal role in advancing the understanding of reaction mechanisms occurring on catalyst surfaces. Grasping the plasma-surface interactions will allow tailoring catalysts to tune plasma-driven catalytic reactions. Nevertheless, existing literature indicates that researchers have only recently explored approaches to introduce plasma in DRIFTS cells. Challenges originating from compact geometry of a DRIFTS cell have prompted scientists to design custom systems to measure the IR signal while simultaneously generating a NTP, either close to the catalyst bed or within the catalyst bed. Because the location of the plasma zone plays a crucial role in how the plasma species interact with the catalyst, thus affecting reaction mechanisms, different system configurations can measure different phenomena, all of which can be applicable to different types of plasma catalysis. For instance, certain systems solely activate the gas phase with NTP, focusing on the interaction of dissociated species with the catalyst. In contrast, others examine how NTP activates the catalyst bed as well. Further, the small size of DRIFTS cells limits the measurement of the injected voltage due to the large size of the probe, so the only NTP parameter commonly reported is the applied voltage. Furthermore, some cells have the capability to be heated and therefore to perform thermocatalytic experiments in the absence of NTP or to combine NTP with thermal catalysis and evaluate the impact of NTP on the reaction mechanisms, as well as to pretreat the catalyst before the reaction. Adding a heating element also presents additional difficulties since plastic components, while they are not electrically conductive, can limit the ability to heat the system. Fig. 2 illustrates DBD DRIFTS cell configurations that will be reviewed in this perspective, while Table 1 summarizes the methodologies and reaction mechanism insights determined using these DBD DRIFTS configurations.



Table 1 Selected list of plasma DRIFTS studies, highlighting main features and scientific observations, as well as improvements and recommendations

| DRIFTS and plasma type | Reaction conditions | Catalyst | Methodology highlights | Gas phase analysis | Ref. |
|---|---|--|--|-----------------------------------|------|
| – <i>Operando</i> DRIFTS-MS | – CH ₄ oxidation | Pd/A ₂ O ₃ | • DRIFTS cell design with embedded catalyst in NTP, simulating tubular DBD. | • MS | 27 |
| – Fixed bed DBD | – Temperature: ambient | | • The system presents no signal interference between IR beam and plasma plume. | | |
| – Generator: AC | – Diluent gas: Ar | | | | |
| – Voltage: 5–6 kV | | | | | |
| – Frequency: 27 kHz | | | | | |
| – <i>Operando</i> DRIFTS | – CO ₂ hydrogenation | Ru/MgAl layered double hydroxide (LDH) | • DRIFTS with embedded catalyst in NTP. | • MS | 28 |
| – Fixed bed DBD | – Temperature: ambient | | • DRIFTS used for studying catalysts validated in tubular DBD. | • OES (not on DRIFTS cell) | |
| – Generator: AC | – Diluent gas: Ar | | • Plasma and products gas phase characterization | | |
| – Voltage: 5.0 kV | | | | | |
| – Frequency: 23.5 kHz | | | | | |
| – <i>Operando</i> DRIFTS | – CO ₂ hydrogenation | Ru/SiO ₂ * | • DRIFTS with embedded catalyst in NTP. | • MS | 29 |
| – Fixed bed DBD | – Temperature: ambient | | • DRIFTS used for studying catalysts validated in tubular DBD. | | |
| – Generator: AC | – Diluent gas: Ar | | | | |
| – Voltage: 5.5 kV | | | | | |
| – Frequency: 27 kHz | | | | | |
| – <i>In situ</i> DRIFTS | – CO ₂ hydrogenation | Fe ₂ O ₃ /γ-Al ₂ O ₃ | • DRIFTS with embedded catalyst in NTP. | • None | 30 |
| – Fixed bed DBD | – Temperature: ambient | | • DRIFTS used for studying catalysts validated in tubular DBD. | | |
| – Generator: AC | – Diluent gas: No | | | | |
| – Voltage: 24 kV | | | | | |
| – Frequency: 9.5 kHz | | | | | |
| – <i>In situ</i> DRIFTS | – No reaction, only Ar | KBr | • Helical surface DBD could improve the synergy plasma-catalyst. | • None | 31 |
| – Helical surface DBD | – Temperature: ambient | | • Adjusting gas and water content in a packed bed enables exploration of different plasma regimes, not feasible at atmospheric pressure. | | |
| – Generator: AC | – Diluent gas: air or Ar | | | | |
| – Voltage: 0.9 kV | | | | | |
| – Frequency: 27 kHz | | | | | |
| – <i>In situ</i> DRIFTS | – CO ₂ hydrogenation | Co/CeZrO ₄ | • DBD above the catalyst bed activating mainly the gas phase. | • None | 32 |
| – DBD over catalyst surface | – Temperature: ambient | | • Possibility of thermally treating the catalyst. | | |
| – Generator: AC | – Diluent gas: No | | • Temperature monitoring with IR and UV-vis. | | |
| – Voltage: 8 kV | | | | | |
| – Frequency: 1 kHz | | | | | |
| – <i>Operando</i> DRIFTS | – Hydrocarbon selective catalytic reduction (HC-SCR) deNO _x reaction | Ag/Al ₂ O ₃ | • DBD above the catalyst bed activating mainly the gas phase. | • MS | 33 |
| – DBD over catalyst surface | | | • Gas temperature determined from the rotational temperature of the nitrogen measured spectroscopically through OES. | • OES for temperature measurement | |
| – Generator: AC | – Temperature: ambient | | | | |
| – Voltage: 4–7.5 kV | – Diluent gas: He | | | | |
| – Frequency: 20 kHz | | | | | |
| – <i>Operando</i> DRIFTS | – CH ₄ decomposition | Ni/Al ₂ O ₃ –SiO ₂ | • Point-source DBD activating mainly the gas phase. | • IR | 34 |
| – DBD over catalyst surface | – Temperature: ambient and 500 °C | | • RF plasma jet. | | |
| – Generator: RF | – Diluent gas: Ar | | | | |
| – Voltage: n.a. | | | | | |
| – Frequency: 14.3 MHz | | | | | |
| – <i>In situ</i> DRIFTS | – CH ₄ dry reforming | Ni/Al ₂ O ₃ | • Point-source DBD activating mainly the gas phase. | • None | 35 |
| – Point source DBD | – Temperature: 200 °C | La–Ni/Al ₂ O ₃ | • <i>Ex situ</i> CO ₂ -TPD to investigate the generation of carbonates at temperatures above 200 °C. | | |
| – Generator: AC | – Diluent gas: He | | | | |
| – Voltage: 5.5 kV | | | | | |
| – Frequency: 0.05 kHz | | | | | |
| – <i>Ex situ</i> DRIFTS | – CO ₂ hydrogenation | Co/Al ₂ O ₃ | • <i>Ex situ</i> DRIFTS to support findings from tubular DBD reactor. | • None | 36 |
| – Samples transferred into the DRIFTS chamber inside a glove box under Ar | | | | | |



2.3 Review of existing custom-made non-thermal plasma DRIFTS configurations

Stere *et al.*²⁷ performed methane (CH₄) oxidation over a Pd/Al₂O₃ catalyst in a fixed bed DBD DRIFTS cell where the power electrode is embedded in the catalyst bed leading to direct plasma–catalyst interactions (Fig. 2a). In this study, the authors were able to observe enhancement in the formation of intermediate species with NTP and proposed different reaction mechanisms for thermal and plasma catalysis pathways. They concluded that thermal conditions favor the carbonate route, while plasma conditions predominantly involve the formate route. The authors did not observe high concentrations of carbonates under NTP, indicating that the decomposition of carbonates into CO₂ was promoted, while the high amount of formate generated during NTP application could arise from reaction of gas phase and surface CO with surface hydroxyl groups (–OH) on Al₂O₃. Additionally, the system is equipped with a downstream MS enabling detection of varying concentrations of CO, CO₂, and CH₄ correlated with the applied voltage. The same system was used by Xu *et al.*^{28,29} in two separate studies for CO₂ hydrogenation over supported Ru catalysts. They observed that the reaction over Ru/MgAl layered double hydroxide (LDH)²⁸ increased CO₂ conversion (~85%) and CH₄ yield (~84%) at ambient temperature compared to conventional thermal catalysis (>250 °C). In addition, the reaction over Ru/SiO₂ showed superior mitigation of CO poisoning in plasma catalysis compared to thermal catalysis, attributed to effective removal of strongly adsorbed carbon species through collisions with species from the plasma, restoring essential active sites for CO₂ activation.²⁹ In both contributions, DRIFTS revealed that plasma activation facilitates the generation of diverse active species in the gas phase and on the catalyst surface, contributing to the enhanced performance of the plasma catalysis system. The authors implemented DRIFTS to support studies performed in tubular DBD reactors, to confirm beneficial plasma–surface interactions on chemical conversion. In addition optical emission spectroscopy (OES) was used to compare the gas phase composition with and without a catalyst in the plasma zone.²⁸

Meng *et al.*³⁰ performed NTP assisted CO₂ hydrogenation to methanol over Fe₂O₃/γ-Al₂O₃ catalyst in a packed bed DRIFTS cell configuration similar to that shown in Fig. 2a. In their investigation they observed a gradual increase in surface carbonates in the presence of NTP, suggesting that the presence of carbonate species is not solely due to the physical adsorption of CO₂. This effect was attributed to plasma excitation, specifically CO₂ vibrational excitation on the catalyst surface. Bicarbonate transformation into formate and the presence of surface bonded CH₃O (denoted from here onward with *) indicated the role of formate as a crucial intermediate in methanol synthesis. The absence of CO, except at high voltage, led to a proposed mechanism involving CO₂ capture by chemisorbed oxygen species, forming CO₃* and facilitating CO₂ hydrogenation *via* the formate pathway. Subsequent events, including CH₃OH desorption, oxygen vacancy emergence, and reverse

water gas shift (RWGS) reactions, contributed to the measured CH₃OH. This study focused on using DRIFTS in a tubular DBD reactor to study the effect of the catalyst, although without characterization of gas phase plasma-activated species or downstream monitoring of products.

In general, the packed bed DBD DRIFTS configuration (Fig. 2a) enables direct interaction of the plasma with the catalyst bed. However, even though there is no signal interference between IR beam and plasma plume, the IR signal may not capture specific transformations occurring at different vertical axis positions, as the beam only reaches the top surface of the catalyst. The advantage of this configuration is that it closely resembles a packed bed tubular DBD reactor, offering enhanced relevance in terms of yield, conversion, and selectivity measurements. In an alternative approach, Turan *et al.*³¹ developed a compact helical surface DBD DRIFTS system, where the helix acts as ground electrode, separated from the inner power electrode by a Kapton dielectric coating, thereby augmenting the plasma contact area with a packed bed (Fig. 2b). The experimental configuration, inclusive of optical and electrical measurements in both unpacked and packed bed systems, demonstrated the adaptable nature of the reactor, operating in either filamentary (discrete plasma) or glow-like (continuous) modes depending on the gas composition. The unintentional introduction of air into the DRIFTS chamber induced a transition from a filamentary to a glow discharge elucidating the consequential impact of water desorption from potassium bromide (KBr) on the plasma characteristics. This result underscores the importance of appropriate pre-treatment or drying of KBr.

In contrast, the configuration employing a tubular DBD reactor that generates plasma above the catalyst bed (Fig. 2c) activates gas phase molecules before they reach the catalyst, confining its engagement with the top layer of the catalyst surface. This modified DRIFTS cell was employed by Parastayev *et al.*³² for CO₂ hydrogenation over a Co/CeZrO₄ catalyst, demonstrating that cobalt (Co) nanoparticles on a CeZrO₄ support allow efficient CO₂ hydrogenation in NTP at ambient conditions. According to their observations, the process involved CO as an intermediate on metallic Co particles, with observed Ce³⁺ formation indicating ceria oxygen vacancies generated by a hydrogen plasma. Notably, hydroxyl generation on the catalyst surface was also observed, and *in situ* temperature monitoring attributed these effects to NTP rather than heating of the catalyst. The mechanism, determined solely based on DRIFTS measurements, proposes that CO₂ activation occurs in the gas phase, leading to CO production that adsorbs on the Co surface where dissociation and hydrogenation proceeded.

A similar system was evaluated by Stere *et al.*,³³ performing hydrocarbon selective catalytic reduction (HC-SCR) deNO_x reaction over Ag/Al₂O₃. The study investigated the conversion of simulated diesel fuels, toluene, and *n*-octane, at low temperatures under NTP conditions. The authors observed the production of isocyanate from *n*-octane, aligning with the established thermal activation process at elevated temperatures. The



results support the enhanced performance of the Ag catalyst in *n*-octane-SCR at low temperatures, with a proposed mechanism similar to thermal activation involving isocyanate as the active intermediate. They also confirmed that the catalyst activity was not influenced by thermal activation caused by gas heating under NTP conditions. The local maximum temperature, measured through rotational gas temperature of nitrogen molecules, was found to be a stable ~ 110 °C at the maximum applied voltage of 7.5 kV. The authors also implemented a downstream MS to track the hydrocarbon generation, but the gas phase chemistry in the plasma was not investigated. In a similar DBD DRIFTS cell, Zhang *et al.*³⁴ performed CH₄ decomposition in Ar and Ar/O₂ mixture over a Ni-supported Al₂O₃/SiO₂ catalyst. The authors observed surface-bound C–O only in the presence of plasma, and the C–O IR signal intensity scales with temperature. However, when the catalyst was exposed to plasma-generated particle fluxes under highly oxidizing conditions, the formation of surface C–O was suppressed. The production of CO and CO₂ *via* plasma-catalytic reactions, measured through a downstream IR, follows the trend of surface C–O bond formation, which becomes significant when transitioning from low to high oxygen plasma conditions at catalyst temperatures of 500 °C. Additionally, the surface-bound CH_{*n*} (*n* = 1, 2, 3) species on the catalyst were analyzed using DRIFTS, revealing a correlation between the destruction of CH_{*n*} species and the formation of C–O bonds. This indicates a potential conversion process from CH_{*n*} to CO in presence of NTP, suggesting a plasma-mediated catalyst regeneration mechanism through interactions between the plasma and catalyst surface.

Sheng *et al.*³⁵ performed CH₄ dry reforming in a point-source DBD reactor cell, wherein the high-voltage needle electrode was positioned above the catalyst powder and the ground electrode at the periphery of the ceramic catalyst holder to generate NTP between the needle and powder (Fig. 2d). This configuration activates molecules in the gas-phase and the NTP interacts mainly with the surface of the catalyst. In their study the CH₄ conversion over Ni/Al₂O₃ and La–Ni/Al₂O₃ catalysts revealed notable differences in their CO₂ adsorption behaviors. Ni/Al₂O₃ exhibited weak absorbance intensity for carbonate species, indicating limited active sites for CO₂ activation at the Ni-nanocrystals/Al₂O₃ interface. In contrast, La–Ni/Al₂O₃ showed stronger and diverse carbonate peaks, suggesting a more active role of the La–Ni/Al₂O₃ system in CO₂ activation. The proposed Langmuir–Hinshelwood mechanism suggests CH₄ dissociatively chemisorbs on Ni as CH₃* and H*, while CO₂ binds to La in La–Ni/Al₂O₃, contributing to CO₃^{2–} formation. During the reforming stages, CO₂ activated in the plasma zone leads to an increase in surface carbonate species. These carbonate species in turn oxidize CH_{*x*}* to form CH_{*x*}O*, leading to syngas (CO and H₂) release into the gas phase. The study suggests that increased carbonate generation by plasma-activated CO₂ can boost surface reactions, promoting the conversion of CH₄. Additionally, an Eley–Rideal mechanism involving vibrationally excited CO₂ reacting with adsorbed CH_{*x*}* is proposed, which could play a role in the formation of syngas.

The previously discussed examples highlight that downstream and gas phase products monitoring could strengthen the proposed reaction mechanisms, especially considering that the NTP predominantly activates gas phase species in this configuration rather than interacting with the catalyst surface. Interestingly the authors observed a correlation between the CH₄ conversion and the amount of carbonate generated which was measured through DRIFTS at 200 °C and through *ex situ* CO₂-TPD at 300–600 °C. A completely different approach was used by Wang *et al.*³⁶ in a recent study on CO₂ hydrogenation over Co/Al₂O₃ where *ex situ* DRIFTS was used to confirm reaction mechanisms proposed after investigating the thermal and NTP reaction in a tubular DBD system. After the reaction, the catalyst was loaded in the DRIFTS cell under Ar and the presence of surface species was evaluated.

The authors were able to observe the presence of long-lived surface species such as bidentate formate, bicarbonate, and monodentate carbonate, but no CO or CH_{*x*} peaks were observed due to their short lifetimes. This approach highlights that it is possible to obtain useful information through an *ex situ* approach, although *in situ* DRIFTS is still needed to provide comprehensive insight into the reaction mechanism as a function of reaction parameters and time.

The final configuration reported in Fig. 2e and Fig. 2e' shows two cross sectional representations of the *operando* DRIFTS system developed by the authors of this work. The NTP is generated above the surface of the catalyst, interacting with the gas phase and with the catalyst surface, and an additional downstream IR is connected to the cell output to measure the reaction products composition. The system has been designed with a tungsten filament encapsulated in a quartz sheath as the power electrode (Fig. 2e'), while the catalyst holder functions as ground electrode. In this configuration, the IR radiation interacts with the catalyst surface that is directly exposed to the NTP discharge, but at the same time the plasma does not interact with the whole catalyst bed. Therefore, as for the system in Fig. 2d, yield and conversion measurements might not be fully accurate due to the partial use of the catalyst, compared to a tubular DBD concept. The system is designed to generate plasma through an AC generator delivering a voltage up to 10 kV and a frequency in the range 1–10 kHz (see ESI† for additional details). Importantly, in this configuration, changing the position of the electrode has a large impact on the main discharge direction and intensity towards the catalyst surface, since the dome is electrically grounded too. Therefore, it is important to visually inspect the correct location to direct the discharge towards the catalyst surface. In addition, our configuration allows heating of the catalyst holder up to 500 °C through an external electric resistance. The actual temperature of the catalyst bed was determined by calibrating the inner temperature using a second thermocouple and measuring the temperature with different gases, flow rates, and catalysts. It is also important to mention that this feature allows direct comparison of NTP and thermal conversion, in addition to performing NTP-assisted thermo-catalysis. Certain reactions, such as the dehydration of bicarbonates and formate during



CO₂ hydrogenation require higher temperatures, as suggested by Parastaev *et al.*³² Therefore, in order to properly design catalysts also for NTP, heating capability is a significant feature. Compared to other configurations previously described, this one requires the use of catalyst in pellet form instead of powder, to avoid particle entrainment due to static charge caused by the electric field between the power electrode and the dome that is in electrical contact with the ground. In general, the needle-plate DBD configurations, illustrated in Fig. 2d–e', have a localized plasma zone on the catalyst surface that is centered around the needle electrode. Therefore, particular attention should be given in aligning the IR beam with the plasma activated surface.

2.4 Complementary analytical techniques

The investigations reported previously highlighted the importance of using DBD DRIFTS to monitor the generation of intermediates on the catalyst surface under reaction conditions. However, the information that can be obtained through this technique is confined to the adsorbate species on the catalyst surface. Further, it is often challenging to assign an IR signature unambiguously to a specific adsorbate species. Therefore, coupling DRIFTS with complementary techniques can provide a more comprehensive picture of chemical reaction pathways, thus moving towards *operando* configurations; an approach often adopted in thermal catalysis as well. In DBD DRIFTS cells, the introduction of additional monitoring equipment is often limited by the relatively small geometry of the DRIFTS cell. Because varying geometries of DBD DRIFTS cells exist, it is paramount to evaluate the effect of plasma configuration on the reaction mechanism proposed, which is best accomplished using multiple analytical techniques. Indeed, the different NTP configurations can affect the surface intermediates due to gas-phase reactions, activation energies, and 2D distributions of radicals/intermediates near the catalyst surface. Fig. 3 summarizes the main techniques we propose to use in conjunction with DRIFTS to elucidate plasma-catalytic reaction mechanisms.

In temperature-programmed desorption (TPD), after adsorption of a molecule of interest, a catalyst is heated, and the desorbed surface species are analyzed *via* MS, for example. From TPD, the activation energy of desorption can be extracted, offering insights into catalytic reaction kinetics and mechanisms.^{37–40} To assess the benefit of energy inputs other than temperature on activation energies, researchers have derived Arrhenius relationships for photo-assisted catalysis,⁴¹ and recently plasma catalysis.^{10,42} Characterizing the gas-phase composition often requires the use of multiple techniques to study both neutral and activated species (such as dissociated molecules or ionized species). Downstream IR, MS, and GC coupled with a detector are commonly used in-line to measure neutral and stable products such as CO, CH₄, CO₂, H₂O, light hydrocarbons and other oxygenates.^{27,29,33} Conversion and product yields can be deduced from these measurements. To identify excited species in the plasma, the emission from radiative decay mechanisms is often unique enough to identify

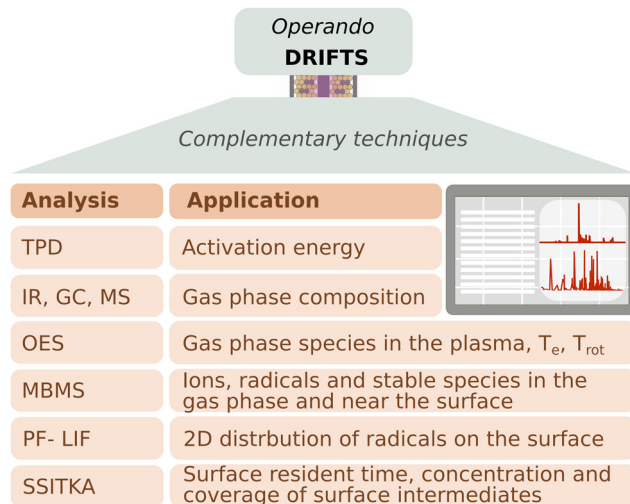


Fig. 3 Scheme highlighting analytical techniques complementary to *operando* DRIFTS: temperature-programmed desorption (TPD), infrared (IR) or mass spectrometry (MS), optical emission spectroscopy (OES), molecular beam mass spectrometry (MBMS), photofragmentation laser-induced fluorescence (PF-LIF), steady-state isotopic transient kinetic analysis (SSITKA).

the associated species and can be measured using OES. OES provides crucial information on ionized intermediates and how the presence of a catalyst alters the gas-phase chemistry in NTP.⁴³ Further, from OES, other plasma-relevant parameters can be extracted. For example, the electron temperature of Ar plasmas can be approximated⁴⁴ and under certain conditions the gas temperature can be extracted from the rotational vibration of a diatomic molecule.⁴⁵ Reaction mechanisms derived from DRIFTS often include assumptions regarding surface intermediates. Steady-state isotopic transient kinetic analysis (SSITKA) is a technique used to identify surface intermediates, their density on the catalyst surface, and their kinetic parameters. The technique involves achieving a steady-state catalytic reaction using an unlabeled reactant mixture followed by switching abruptly to an isotope-labeled mixture, without disrupting the steady state of the reaction. This transition does not alter the overall product formation rate or the surface chemical composition, but allows for the determination of surface residence time, and concentration and coverage of dominant surface intermediates.^{46,47}

In contrast, molecular beam mass spectrometry (MBMS) has been found to be beneficial for observing the generation of species in the gas phase and near the catalyst surface, measuring radicals, ions, and stable molecules, and also their evolution over time, which is critical for understanding kinetics and reaction pathways.^{48–51} For example, Gurses *et al.*⁵⁰ combined *operando* DRIFTS studies and near-surface MBMS (ns-MBMS) to investigate the formation of C₂ oxygenates during methanol oxidation catalysis on MgO-supported Pd at atmospheric pressure. The observation of the oxygenates contributed to an enhanced understanding of the fate of surface CH₂O, elucidating the desorption process, spillover, and reaction with surface oxygenates, thus deepening insights into C₂ product



generation. Their study also indicates that although there are methoxy and formate species on the surface, it is the presence of the dioxymethylene group in near-surface methoxymethanol that suggests the transient presence of formaldehyde, undetectable by DRIFTS only. Therefore, the MBMS complemented the reaction mechanism, highlighting the importance of formaldehyde as a building block for desorbing C₂ oxygenates. Burger *et al.*,⁵¹ used MBMS coupled with a DBD reactor to study low temperature methane oxidation on CuO. Mechanistic insights were obtained by quantifying the fuel oxidation, stable intermediate species, and CO₂ production, generating a reaction mechanism, while also observing the positive impact of plasma in reducing the oxidation temperature by 200 °C. On the other hand, MBMS can be used to detect reactive radicals as investigated by Zhang *et al.*⁴⁸ in their work on plasma-assisted oxidation and pyrolysis of methane. They were able to link the observed radicals (CH₂, CH₃, O) and stable molecules (CH₄, CO, O₂, Ar) with the generation of C₂–C₅ hydrocarbons, confirming the possibility of measuring NTP excited species through MBMS. Another technique used to study radicals is photo-fragmentation laser-induced fluorescence (PF-LIF). It has been implemented to characterize local 2D distributions of CH₃*⁵² or OH* and H₂O₂*⁵³ providing important additional information on how species evolve close to the catalyst surface.

2.5 Recommendations for DRIFTS usage in plasma catalysis

Operando DRIFTS for plasma catalysis has proven very useful because of the intrinsically dynamic and transient nature of plasma-driven processes. Therefore, an *operando* system enables the time-dependent monitoring of surface intermediates under varying reaction conditions, including plasma discharge parameters and reaction products. However, the introduction of a catalyst into a plasma discharge zone affects the plasma itself, and *vice versa*. One of the major knowledge gaps in plasma catalysis is the understanding of plasma-catalyst interactions. We recommend studying the impact of plasma on surface reactions sequentially: (a) evaluating the catalyst in the absence of a plasma (thermal only), (b) during plasma application, and (c) then in the absence of a plasma again (thermal only), as well as in the reverse sequence, *i.e.*, plasma-thermal-plasma. These consecutive tests should be performed with the same catalyst load, reducing the catalyst between each experiment to remove species formed on the surface. This approach would generate comparative data on the same catalyst sample, minimizing the error caused by introducing a different catalyst sample that might have different surface characteristics.

Sample preparation is another important step to consider as it impacts the reliability of the data. In our system (Fig. 2e and e'), a pelletized catalyst is necessary to avoid static charging and attraction of particulates towards the metal dome, but the other systems (Fig. 2a–d) can be used with a powder catalyst. However, even when catalyst powder is used, there may be inconsistencies between experiments, leading to differences in peak intensities. These inconsistencies could be due, for example, to subtle changes in catalyst bed surface topology caused by

particles entrained by the gas flow, thereby impacting the interaction of the IR beam with the catalyst. Hence, even though DRIFTS provides essential data for catalyst design, it requires complementary methods to deeply understand reaction mechanisms.⁴ Each DRIFTS system has advantages and disadvantages, and it is important to critically assess the results even when performing the same reaction with the same conditions and catalysts, because the impact of plasma discharge interactions can dramatically change the catalytic performance and characterization of relevant species. On one hand, if catalyst development is the focus, the configuration shown in Fig. 2a might represent the best option to simulate a catalyst fully immersed in a plasma zone, as it is often the case in larger scale tubular DBD reactors. This DRIFTS configuration also allows measurement of yields for a given hourly space velocity. In this configuration, however, the IR beam detects only the surface species at the top of the catalyst bed and doesn't provide information about surface intermediates deeper into the catalyst bed. A maximized interaction between the plasma and the top surface of the catalyst material could be obtained by extending the length of the electrode slightly above the catalyst surface. The other configurations with plasma discharge partially or completely separated from the catalysts allow measurement of the catalyst interaction with species dissociated or vibrationally excited in the gas phase. In this case NTP interaction is limited only to a portion of the catalyst, and an overall lower energy transfer to adsorbates in the catalyst bulk is expected. For this reason, depending on the species of interest, one configuration might be more appropriate than the other, considering that NTP embedded with the catalyst bed could allow for analysis of short life excited species. On the other hand, plasma generated outside the catalyst bed can enable investigation of how dissociated species in the gas phase interact with the catalyst.

DRIFTS is usually used as a supporting technique to perform mechanistic studies coupled with catalytic performance studies in a larger scale reactor (*e.g.* tubular DBD reactor). However, the plasma discharge and synergy with the catalyst is strongly dependent on the geometry and reactor configuration. Therefore, it would be also beneficial to report different performances between DRIFTS cells and a larger scale reactor. Furthermore, to ascribe a mechanism obtained from DRIFTS to a reaction occurring in a reactor separate from the DRIFTS chamber, it is important to match the same discharge conditions in terms of power and frequency in both plasma discharges. Because different circuit impedances may arise due to different reactor geometries, we recommend measuring injected power in both configurations if possible. Additionally, it is strongly recommended to clearly report details of DRIFTS procedures used.

In order to clarify the impact of reporting experimental details, we performed plasma CO₂ hydrogenation over a traditional Fischer-Tropsch catalyst, Co/Al₂O₃,^{54–56} in our *operando* DBD DRIFTS (Fig. 2e and e') system. Details of the experimental procedure are reported in the ESI.† The DRIFT spectra obtained at 20 °C and 350 °C are shown in Fig. 4a–d, respectively. The



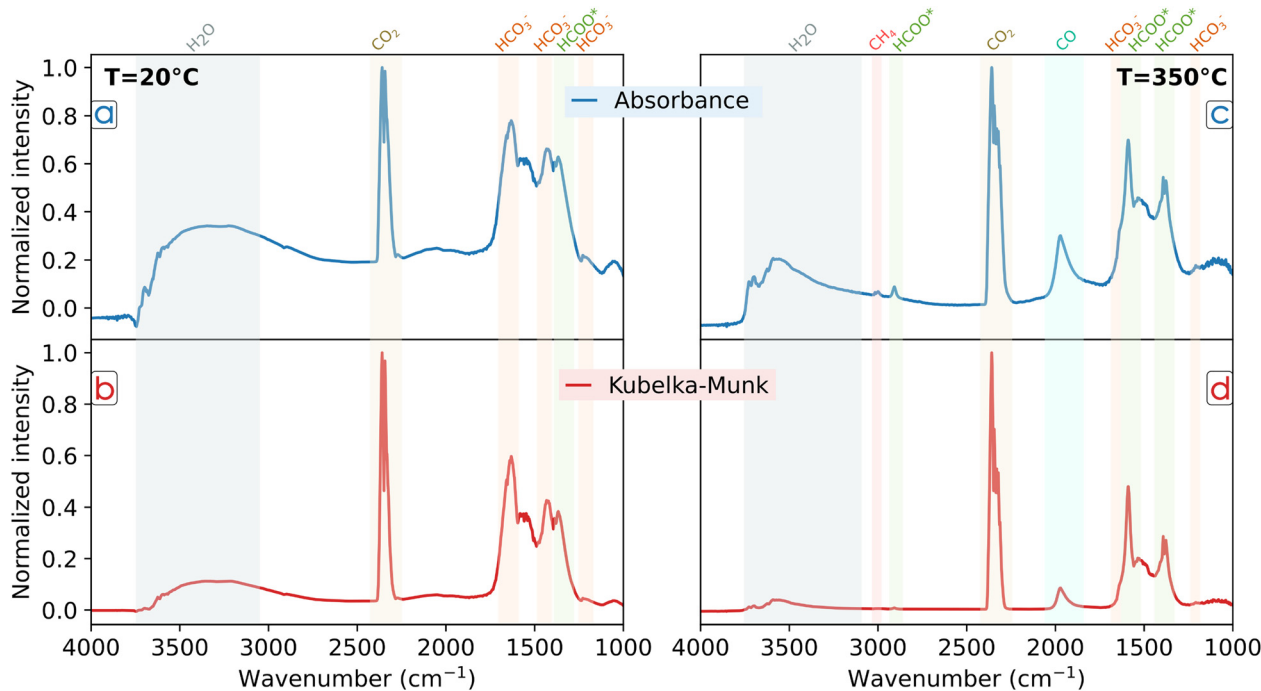


Fig. 4 Comparison of absorbance vs. Kubelka–Munk spectra taken during NTP CO₂ hydrogenation over Co/Al₂O₃. The DRIFTS cell temperature was controlled at 20 °C (a) and (b), and 350 °C (c) and (d). Data were collected in a custom modified DBD DRIFTS cell at 4000 V and 10 kHz with 36 sccm of Ar, 1 sccm of CO₂, and 3 sccm of H₂.

data was processed in terms of absorbance ($\log(1/R)$) and compared with the K–M transform, where the peak intensity was normalized to the gas-phase CO₂ signal. Since K–M is most representative of highly absorbing catalysts, the correct choice of data processing methodology could depend on the catalyst Co loading and considering the two methods could be beneficial. In general, both K–M and absorbance spectra show peaks in same positions for each temperature, but differences in Fig. 4a–d can be noted. At low temperature, the broad and intense band around 3500 cm⁻¹ corresponding to water, is clearly visible in both cases, but with stronger intensity in the absorbance spectrum. Regarding the peaks in the lower energy region, bicarbonate (HCO₃⁻) was identified by characteristic bands at 1230, 1442 and 1646 cm⁻¹, representing respectively the $\nu_{\text{as}}(\text{C}-\text{O})$ asymmetric stretching frequency, the $\delta(\text{O}-\text{C}-\text{O})$ bending mode and the $\nu_{\text{s}}(\text{C}=\text{O})$ symmetric stretching frequency.^{24,57,58} The bands at 1378 and 1392 cm⁻¹ can be associated with the presence of formate (HCOO*) and the $\nu_{\text{s}}(\text{C}-\text{O})$ symmetric stretching frequency and the $\delta(\text{C}-\text{H})$ bending mode, respectively. When processing the measurements with K–M function (in Fig. 4b), the relative intensity to CO₂ of each peak is lower. These species are mainly absorbed over the alumina surface and the K–M function transforms the IR signal into a low-intensity peak. This effect is even more noticeable at higher temperatures. The spectrum collected during reaction at 350 °C (Fig. 4c) shows lower intensity bands for bicarbonates due to desorption and the dehydration reaction yielding formate. Indeed, the absorbance spectrum shows stronger signal of HCOO*, where, in addition to the peaks at 1378 and

1392 cm⁻¹, two additional peaks are strongly visible at 1592 and 2900 cm⁻¹ representing the $\nu_{\text{as}}(\text{C}-\text{O})$ asymmetric stretching frequency and the $\nu_{\text{as}}(\text{C}-\text{H})$ asymmetric stretching frequency, respectively.^{22–24,26,59} In addition, the band at ~ 2000 cm⁻¹ can be associated with CO adsorbed on metallic Co sites,^{13,60} while the peak at 3014 cm⁻¹ represents gas phase CH₄ as it desorbs from the catalyst surface.^{10,61} In this case, when applying the K–M transformation (Fig. 4d), information could be lost due to the lower intensities of the CH₄ and CO peaks. Indeed, these species are weakly bonded to the catalyst metal sites in comparison to HCO₃⁻ and HCOO* on the alumina, resulting in a limited capacity of K–M to highlight the presence of important intermediates formed over the catalyst surface. Therefore, it is very important to specify which method was used when presenting and reporting data to the scientific community.

When performing DRIFTS experiments it is also critical to clearly specify how the background was measured. Temperature and plasma can strongly affect the background. Fig. S1 (ESI[†]) shows the change in the background after 3 hours under Ar plasma (4000 V and 10 kHz), while Fig. S2 (ESI[†]) reports the change in the background measured under same plasma conditions but varying the temperature between 20 °C and 350 °C. In general, background variations may be affected by different factors. Temperature conditions can lead to variations in the concentration and distribution of surface species, which can influence the background signal observed in DRIFTS spectra, for example water in Fig. 4a and c, respectively. Physical changes due to thermal expansion of catalyst material could



impact the optical properties of the sample. Additionally, when striking a plasma at ambient temperature, the background change can be related to similar phenomena, especially to increased temperatures (≤ 180 °C) from electron excitation and impact with catalyst surface, as suggested by Parastaeu *et al.*³² A possible solution is to first record a background for each thermal and plasma condition, and then perform the measurements using the associated background. Additionally, for NTP-assisted thermocatalysis studies where the temperature is increased incrementally, another approach is to collect a background spectrum at the end of each temperature increase in order to evaluate the differences in adsorbate formation between two temperatures. Overall, it is essential to report the timespan between the background collection and the actual measurement, the gas flow rate used for the background collection and experiment, and to report if new backgrounds were collected before every measurement. Regardless of the DRIFTS cell design and procedure, to fully understand and validate the reaction mechanisms, additional analytical techniques are needed to complement observations of surface adsorbates. These are crucial to gather information on the plasma gas phase characteristics as well as reaction occurring in the gas phase and near the catalyst surface.

3. Conclusions

DRIFTS represents a powerful tool for probing reaction mechanisms under thermal and plasma conditions. The review of existing DBD DRIFTS systems reveals diverse configurations employed for plasma catalysis studies, each with their own advantages and limitations. Using NTP modified *in situ* and *operando* DRIFTS systems, these studies have successfully correlated the formation of intermediates on the catalyst surface with the generation of reaction products, in the presence and absence of NTP, leading to an understanding of the impact of NTP excited species as well as the interaction with the catalyst. These efforts highlighted the importance of this technique to draw useful conclusions for catalyst design in plasma catalysis (*e.g.*, observing different pathways in presence of NTP). However, DRIFTS is highly sensitive to experimental conditions, and it is challenging to achieve quantitative results, underscoring the need for careful spectra interpretation. Moreover, our NTP *operando* DRIFTS system showed the importance of DRIFTS data reporting, considering, for example, the loss of information when using K–M function or the drastic changes in the background due to temperature and plasma. Consequently, it is important to properly report the DRIFTS procedure in terms of background collection, methodology (*e.g.*, absorbance, K–M) and sample preparation.

Currently, there is still lack of standardization related to custom-made DRIFTS cells, and cross studies and collaborations between experts could provide important advancements in the field. Round Robin experiments, where multiple laboratories independently perform experiments using standardized protocols and share results, could play a pivotal role in

addressing this lack of standardization. Furthermore, important information related to catalyst and reactor design could be addressed by understanding the fundamental differences when the same reactions are performed with different plasma discharge modes. Additionally, *operando* systems and complementary analytical techniques, including TPD, downstream IR or MS, OES, SSITKA, MBMS and PF-LIF play a crucial role in obtaining a comprehensive understanding of reaction pathways, providing insights into gas-phase reactions, activation energies, and intermediate species on the catalyst surface. Overall, the integration of DRIFTS with complementary techniques and the systematic exploration of experimental parameters contribute to a more comprehensive and nuanced understanding of catalytic processes, paving the way for designing novel materials and therefore advancing in sustainable and efficient chemical transformations *via* NTP.

Data availability

The data that support results from our work, in Fig. 2e and e', are available from the corresponding author.

Conflicts of interest

There are no conflicts to declare.

Acknowledgements

This work was authored by the National Renewable Energy Laboratory (NREL), operated by Alliance for Sustainable Energy, LLC, for the U.S. Department of Energy (DOE) under Contract No. DE-AC36-08GO28308. This work was supported by the Laboratory Directed Research and Development (LDRD) Program at NREL. The views expressed in the article do not necessarily represent the views of the DOE or the U.S. Government. The U.S. Government retains and the publisher, by accepting the article for publication, acknowledges that the U.S. Government retains a nonexclusive, paid-up, irrevocable, worldwide license to publish or reproduce the published form of this work, or allow others to do so, for U.S. Government purposes.

References

- 1 A. Bogaerts, X. Tu, J. C. Whitehead, G. Centi, L. Lefferts, O. Guaitella, F. Azzolina-Jury, H.-H. Kim, A. B. Murphy, W. F. Schneider, T. Nozaki, J. C. Hicks, A. Rousseau, F. Thevenet, A. Khacef and M. Carreon, *J. Phys. D: Appl. Phys.*, 2020, **53**, 443001.
- 2 R. G. Grim, Z. Huang, M. T. Guarnieri, J. R. Ferrell, L. Tao and J. A. Schaidle, *Energy Environ. Sci.*, 2020, **13**, 472–494.
- 3 A. Piel, *Plasma Physics*, Springer Berlin Heidelberg, Berlin, Heidelberg, 2010, pp. 323–350.
- 4 R. Snoeckx and A. Bogaerts, *Chem. Soc. Rev.*, 2017, **46**, 5805–5863.



- 5 I. Adamovich, S. D. Baalrud, A. Bogaerts, P. J. Bruggeman, M. Cappelli, V. Colombo, U. Czarnetzki, U. Ebert, J. G. Eden, P. Favia, D. B. Graves, S. Hamaguchi, G. Hieftje, M. Hori, I. D. Kaganovich, U. Kortshagen, M. J. Kushner, N. J. Mason, S. Mazouffre, S. M. Thagard, H.-R. Metelmann, A. Mizuno, E. Moreau, A. B. Murphy, B. A. Niemira, G. S. Oehrlein, Z. L. Petrovic, L. C. Pitchford, Y.-K. Pu, S. Rauf, O. Sakai, S. Samukawa, S. Starikovskaia, J. Tennyson, K. Terashima, M. M. Turner, M. C. M. van de Sanden and A. Vardelle, *J. Phys. D: Appl. Phys.*, 2017, **50**, 323001.
- 6 J. Slaets, B. Loenders and A. Bogaerts, *Fuel*, 2024, **360**, 130650.
- 7 S. Meng, S. Li, S. Sun, A. Bogaerts, Y. Liu and Y. Yi, *Chem. Eng. Sci.*, 2024, **283**, 119449.
- 8 P. Atkins, J. de Paula and J. Keeler, *Atkins' Physical Chemistry*, Oxford University Press, 12th edn, 2022.
- 9 J. C. Whitehead, *Front. Chem. Sci. Eng.*, 2019, **13**, 264–273.
- 10 Y. Sun, J. Wu, Y. Wang, J. Li, N. Wang, J. Harding, S. Mo, L. Chen, P. Chen, M. Fu, D. Ye, J. Huang and X. Tu, *JACS Au*, 2022, **2**, 1800–1810.
- 11 V. R. Anderson, N. Leick, J. W. Clancey, K. E. Hurst, K. M. Jones, A. C. Dillon and S. M. George, *J. Phys. Chem. C*, 2014, **118**, 8960–8970.
- 12 N. Biliškov, *Phys. Chem. Chem. Phys.*, 2022, **24**, 19073–19120.
- 13 L. Lukashuk, N. Yigit, R. Rameshan, E. Kolar, D. Teschner, M. Hävecker, A. Knop-Gericke, R. Schlögl, K. Föttinger and G. Rupprechter, *ACS Catal.*, 2018, **8**, 8630–8641.
- 14 T. Bauer, S. Maisel, D. Blaumeiser, J. Vecchiotti, N. Taccardi, P. Wasserscheid, A. Bonivardi, A. Görling and J. Libuda, *ACS Catal.*, 2019, **9**, 2842–2853.
- 15 A. Martínez-Arias, A. B. Hungria, M. Fernández-García, A. Iglesias-Juez, J. Soria, J. C. Conesa, J. A. Anderson and G. Munuera, *Phys. Chem. Chem. Phys.*, 2012, **14**, 2144–2151.
- 16 M. A. Bañares and M. Daturi, *Catal. Today*, 2023, **423**, 114255.
- 17 S. Zhang and G. S. Oehrlein, *J. Phys. D: Appl. Phys.*, 2021, **54**, 213001.
- 18 Y. Zhu, J. Wang, H. Chu, Y.-C. Chu and H. M. Chen, *ACS Energy Lett.*, 2020, **5**, 1281–1291.
- 19 T. Armaroli, T. Bécue and S. Gautier, *Oil Gas Sci. Technol.*, 2004, **59**(2), 215–237.
- 20 M. O. Guerrero-Pérez and G. S. Patience, *Can. J. Chem. Eng.*, 2020, **98**, 25–33.
- 21 J. D. Jimenez, C. Wen and J. Lauterbach, *Catal. Sci. Technol.*, 2019, **9**, 1970–1978.
- 22 Y. Fu, L. Kraus and H. Knözinger, *J. Mol. Catal.*, 1989, **52**, 113–127.
- 23 D. Lorito, A. Paredes-Nunez, C. Mirodatos, Y. Schuurman and F. C. Meunier, *Catal. Today*, 2016, **259**, 192–196.
- 24 X. Wang, H. Shi, J. H. Kwak and J. Szanyi, *ACS Catal.*, 2015, **5**, 6337–6349.
- 25 S. M. Fehr, K. Nguyen and I. Krossing, *ChemCatChem*, 2022, **14**, e202101500.
- 26 L. Proaño, E. Tello, M. A. Arellano-Trevino, S. Wang, R. J. Farrauto and M. Cobo, *Appl. Surf. Sci.*, 2019, **479**, 25–30.
- 27 C. Stere, S. Chansai, R. Gholami, K. Wangkawong, A. Singhanian, A. Goguet, B. Inceesungvorn and C. Hardacre, *Catal. Sci. Technol.*, 2020, **10**, 1458–1466.
- 28 S. Xu, S. Chansai, Y. Shao, S. Xu, Y. Wang, S. Haigh, Y. Mu, Y. Jiao, C. E. Stere, H. Chen, X. Fan and C. Hardacre, *Appl. Catal., B*, 2020, **268**, 118752.
- 29 S. Xu, S. Chansai, S. Xu, C. E. Stere, Y. Jiao, S. Yang, C. Hardacre and X. Fan, *ACS Catal.*, 2020, **10**, 12828–12840.
- 30 S. Meng, L. Wu, M. Liu, Z. Cui, Q. Chen, S. Li, J. Yan, L. Wang, X. Wang, J. Qian, H. Guo, J. Niu, A. Bogaerts and Y. Yi, *AIChE J.*, 2023, **69**, e18154.
- 31 N. Turan, P. M. Barboun, P. K. Nayak, J. C. Hicks and D. B. Go, *J. Phys. D: Appl. Phys.*, 2020, **53**, 275201.
- 32 A. Parastaev, N. Kosinov and E. J. M. Hensen, *J. Phys. D: Appl. Phys.*, 2021, **54**, 264004.
- 33 C. E. Stere, W. Adress, R. Burch, S. Chansai, A. Goguet, W. G. Graham and C. Hardacre, *ACS Catal.*, 2015, **5**, 956–964.
- 34 S. Zhang, Y. Li, A. Knoll and G. S. Oehrlein, *J. Phys. D: Appl. Phys.*, 2020, **53**, 215201.
- 35 Z. Sheng, H.-H. Kim, S. Yao and T. Nozaki, *Phys. Chem. Chem. Phys.*, 2020, **22**, 19349–19358.
- 36 J. Wang, X. Wang, M. S. AlQahtani, S. D. Knecht, S. G. Bilén, W. Chu and C. Song, *Chem. Eng. J.*, 2023, **451**, 138661.
- 37 K. Hashimoto, T. Masuda and T. Mori, in *Studies in Surface Science and Catalysis*, eds. Y. Murakami, A. Iijima and J. W. Ward, Elsevier, 1986, vol. 28, pp. 503–510.
- 38 D. Holmes Parker, M. E. Jones and B. E. Koel, *Surf. Sci.*, 1990, **233**, 65–73.
- 39 G. Munteanu and E. Segal, *Thermochim. Acta*, 1985, **89**, 187–194.
- 40 C. Pirola and A. Di Michele, *Can. J. Chem. Eng.*, 2020, **98**, 1115–1123.
- 41 K. Lorber and P. Djinović, *iScience*, 2022, **25**, 104107.
- 42 A. Parastaev, W. F. L. M. Hoeben, B. E. J. M. van Heesch, N. Kosinov and E. J. M. Hensen, *Appl. Catal., B*, 2018, **239**, 168–177.
- 43 T. L. Van Surksun and E. R. Fisher, *J. Phys. Chem. C*, 2021, **125**, 3924–3939.
- 44 X.-M. Zhu and Y.-K. Pu, *J. Phys. D: Appl. Phys.*, 2010, **43**, 403001.
- 45 P. J. Bruggeman, N. Sadeghi, D. C. Schram and V. Linss, *Plasma Sources Sci. Technol.*, 2014, **23**, 023001.
- 46 M. Jabłońska, *ChemCatChem*, 2021, **13**, 818–827.
- 47 A. Holmen, J. Yang and D. Chen, in *Springer Handbook of Advanced Catalyst Characterization*, Springer, Cham, 2023, pp. 935–965.
- 48 R. Zhang, H. Liao, J. Yang, X. Fan and B. Yang, *Proc. Combust. Inst.*, 2019, **37**, 5577–5586.
- 49 J. Jiang, Y. Luo, A. Moldgy, Y. Aranda Gonzalvo and P. J. Bruggeman, *Plasma Processes Polym.*, 2020, **17**, 1900163.
- 50 S. M. Gurses, N. Felvey, L. R. Filardi, A. J. Zhang, J. Wood, K. van Benthem, J. H. Frank, D. L. Osborn, N. Hansen and C. X. Kronawitter, *Chem Catal.*, 2023, **3**, 100782.
- 51 C. M. Burger, N. Hansen, A. J. Zhang and Y. Ju, *Proc. Combust. Inst.*, 2023, **39**, 5551–5560.



- 52 D. van den Bekerom, C. Richards, E. Huang, I. Adamovich and J. H. Frank, *Plasma Sources Sci. Technol.*, 2022, **31**, 095018.
- 53 D. van den Bekerom, M. M. Tahiyat, E. Huang, J. H. Frank and T. I. Farouk, *Plasma Sources Sci. Technol.*, 2023, **32**, 015006.
- 54 C. G. Visconti, L. Lietti, E. Tronconi, P. Forzatti, R. Zennaro and E. Finocchio, *Appl. Catal., A*, 2009, **355**, 61–68.
- 55 K. Shimura, T. Miyazawa, T. Hanaoka and S. Hirata, *Appl. Catal., A*, 2014, **475**, 1–9.
- 56 A. Lillebø, E. Rytter, E. A. Blekkan and A. Holmen, *Ind. Eng. Chem. Res.*, 2017, **56**, 13281–13286.
- 57 H. Wijnja and C. P. Schultness, *Spectrochim. Acta, Part A*, 1999, **55**, 861–872.
- 58 N. D. Parkyns, *J. Chem. Soc.*, 1969, (A), 410–417.
- 59 X. Wang, Y. Hong, H. Shi and J. Szanyi, *J. Catal.*, 2016, **343**, 185–195.
- 60 T. Das and G. Deo, *J. Mol. Catal. A: Chem.*, 2011, **350**, 75–82.
- 61 A. Westermann, B. Azambre, M. C. Bacariza, I. Graça, M. F. Ribeiro, J. M. Lopes and C. Henriques, *Appl. Catal., B*, 2015, **174–175**, 120–125.

